



Development of laser-driven quasi-monoenergetic proton beam line for radiobiology

A. Yogo^{a,*}, T. Maeda^{a,b}, T. Hori^a, H. Sakaki^a, K. Ogura^a, M. Nishiuchi^a, A. Sagisaka^a, P.R. Bolton^a, M. Murakami^b, S. Kawanishi^a, K. Kondo^a

^a Photo-Medical Research Center, Japan Atomic Energy Agency, Kyoto 619-0215, Japan

^b Hyogo Ion Beam Medical Center, Hyogo 679-5165, Japan

ARTICLE INFO

Available online 24 December 2010

Keywords:

Laser ion acceleration
Medical application of laser-driven particle beams

ABSTRACT

We report the development of a laser-driven quasi-monoenergetic proton beamline for the purpose of cell samples irradiation. Laser pulses are focused to an intensity of 5×10^{19} W/cm² onto a polyimide foil target of 7.5- μ m thickness. The emitted proton spectrum is continuous up to a maximum energy of 4 MeV. Energy selection for transport to cancer cells is determined by four pairs of dipole magnets, which consists of a pair of permanent magnets generating a central magnetic field of 0.78 T. Protons are steered by the first magnetic field, and again by the second one, such that transmitted proton trajectories in the middle of the four dipoles are shifted laterally from the target normal axis by an energy-dependent displacement. Proton energy is selected by a pinhole in this middle plane and subsequently steered downstream by the other two dipole magnets. We have obtained 2.25 MeV proton beams with an energy spread of 0.66 MeV (FWHM) and single bunch duration of 20 ns. The dose given in a single proton bunch was 0.2 Gy, hence, the single bunch dose rate is estimated to be 10^7 Gy/s. At the 1 Hz repetition-rate cell samples were irradiated with successive proton bunches with integrated dose levels up to 8 Gy.

© 2010 Elsevier B.V. All rights reserved.

1. Introduction

It has been widely recognized that the use of particle ion beams in cancer radiotherapy has the physical advantage of delivering longitudinally a more localized dose deposition associated with the well-known Bragg peak phenomenon [1]. Further benefit of the ion beam radiotherapy (IBRT) is based on the increased relative biological effectiveness (RBE) within the Bragg peak region [2]. To date, more than 52,000 patients have treated by ion beams at 25 institutes all around the world. However, the high capital cost of IBRT facilities remains a primary hurdle to a more widespread access to this treatment modality. Recently, high-intensity laser acceleration has been suggested as a potential, cost-saving alternative technology [3] to conventional ion accelerators for radiotherapy.

A unique feature of laser acceleration is the extremely-high peak current attributed mostly to the short duration of a single proton bunch. We reported the first demonstration of DNA double-strand breaking of human cancer cells by laser-driven proton bunches of short duration and high single bunch current [4]. Several investigations have subsequently reported radiobiological effects of high dose rate irradiation by laser-accelerated protons [5–7].

Experimental studies [4–6] to date have used protons with a large energy spread which is characteristic of laser-accelerated ions at the source (laser target). While it has been demonstrated that transport line optics downstream of the ion source are energy-selective and can consequently deliver quasi-monoenergetic beams [8], such beam lines have not yet been applied to radiobiological studies. Quantitative evaluation radiobiological effects critically require quasi-monoenergetic irradiation.

To address the problem above, we have developed a laser-driven quasi-monoenergetic proton beamline that consists of sets of miniature permanent magnets. In this paper, we describe a precise setup of the beamline and results of generating 2.25 MeV proton beams with an energy spread of 0.66 MeV (FWHM) and single bunch duration of 20 ns.

The J-KAREN Ti:sapphire laser system [9] at JAEA provided the intense laser pulses for target irradiation. J-KAREN is a femtosecond high-intensity laser system that combines both Ti:sapphire chirped pulse amplification (CPA) and optical parametric CPA (OPCPA) techniques. The system consists of two successive CPA stages, where the second one includes a three-pass Ti:sapphire final booster amplifier pumped with the second harmonic from a high-energy Nd:glass laser. Prior to the peak of the main femtosecond pulse the contrast exceeds 10^{10} on the subnano-second time scale, and is near 10^{12} on the nanosecond time scale. For the present study, laser pulses were delivered to the experiment chamber at a repetition rate of 1 Hz and the final booster amplifier

* Corresponding author.

E-mail address: yogo.akifumi@jaea.go.jp (A. Yogo).

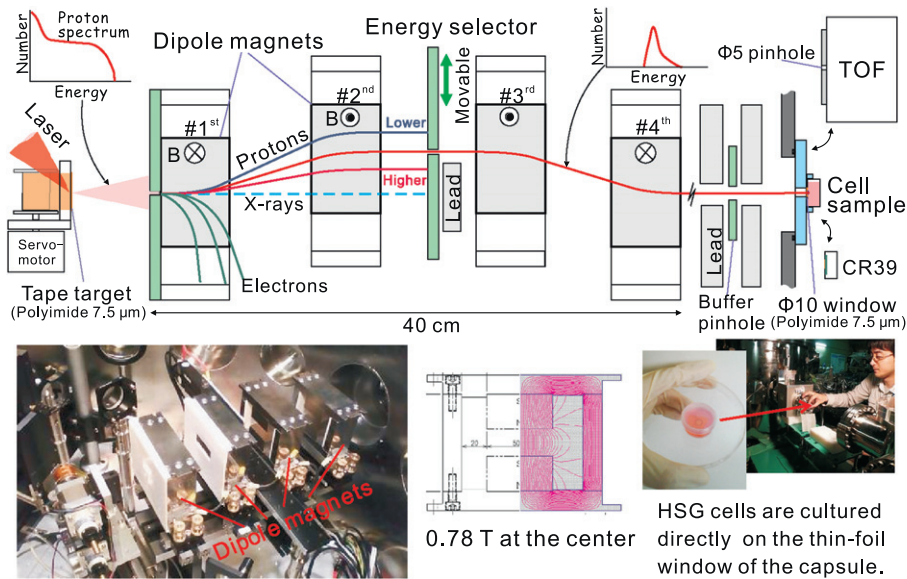


Fig. 1. Experimental setup of the laser-driven quasi-monoenergetic beam line.

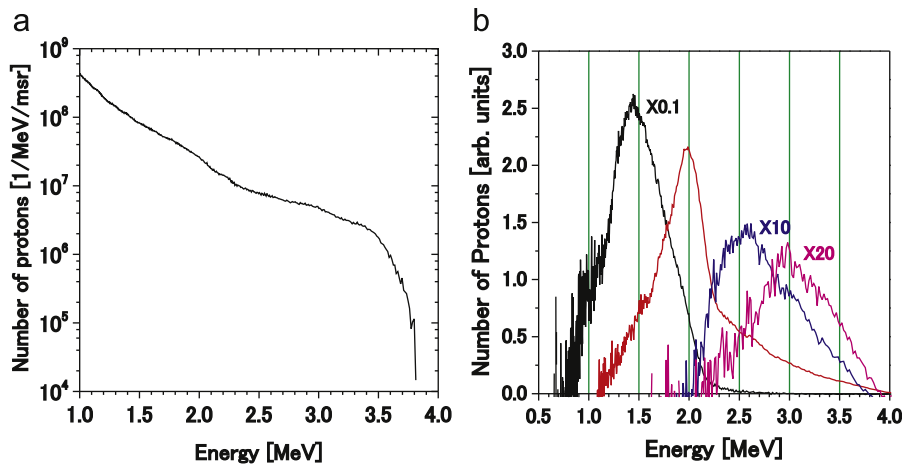


Fig. 2. (a) The proton-energy spectrum obtained without the dipole magnets. (b) Results of beam-energy selection by the four dipole magnets observed with a TOF spectrometer for different energy tunes.

was not used. The configuration of the irradiation system is seen in Fig. 1. Laser pulses of 1 J energy and 45 fs duration are focused to an intensity of $\sim 5 \times 10^{19}$ onto a polyimide target foil of 7.5- μm -thick. Compatible with the 1 Hz laser repetition-rate a new target area is provided for each pulse by advancing the foil tape with a servomotor. At the foil source the initial proton spectrum is continuous with a 4 MeV maximum kinetic energy, as shown in Fig. 2(a).

The proton beam line consists of four dipole magnets, described by Luo et al. [10] in their design of therapy machine. Each dipole magnet consists of a pair of rectangular permanent magnets, generating a central magnetic field of 0.78 T. The second and third magnetic fields are parallel with each other and oriented antiparallel to the first and fourth ones. Protons are collimated by an entrance pinhole and laterally displaced from the target normal axis in the midplane (midway between the second and third magnets) by the first two magnets. Proton energy and energy spread is set by a movable 5 mm diameter pinhole that is located in this midplane. The final two magnets steer protons back to the target normal axis. The transverse beam profile is adjusted by a pinhole. Protons are finally extracted from vacuum into air through a thin polyimide window of 7.5- μm -thickness and 10 mm diameter.

As seen in Fig. 1, the capsule of cell samples is located close to the vacuum window. The cell capsules used during the irradiation were specially designed for our experiments. The capsule (30 mm in diameter) consisted of a vessel and a lid made of heat-resistant plastic, which were sterilized with an autoclave. Beam irradiation enters through the 7 mm diameter aperture on the bottom. Cell samples are cultured on a polyimide cell dish of 7.5- μm thickness at the bottom of the capsule. To irradiate these cells protons must pass through the first 7.5- μm -thick polyimide vacuum window, 3-mm of laboratory air and the 7.5- μm -thick cell dish, keeping their kinetic energy to be high enough to penetrate the cell monolayer.

2. Beam energy tunes

The proton energy spectrum transported through the beam line is measured with online single bunch Time-of-Flight (TOF) spectrometry [11]. The TOF detector is a plastic scintillator (42 mm in diameter) with an upstream 5-mm diameter collimator to duplicate the cell capsule aperture. Fig. 2(b) shows the tunable quasi-monoenergetic proton spectra transported through the beam line.

The central energy could be tuned from 1.5 to 3 MeV by moving the midplane pinhole position laterally between 22 and 10 mm from the target normal axis. The 2.25-MeV protons were used for cell irradiation.

To assess the shot-to-shot fluctuation of single bunch current we recorded TOF spectra for 20 successive laser shots before and after cell irradiation on a single day as seen in Fig. 3(a) and (b), respectively, (single-shot spectra are individually shown in gray and the averaged spectrum is displayed in black). The shot-to-shot reproducibility of spectral shape is reasonable at 1 Hz. The energy spread of the averaged spectrum is 0.66 MeV (full width at half maximum, FWHM). The variation (standard deviation, σ_{fluc}) of proton number over 20 shots is 12.9% and 12.3% in Fig. 3(a) and (b), respectively. This is attributed to the short term stability of the laser intensity. Over the duration of one measurement cycle (that included irradiation of 14 samples and CR-39 measurements) the proton number of the averaged spectra of Fig. 3(a) and (b) reveal a longer term drift of 10.5%.

The areal distribution of protons was observed before and after cell irradiation with CR-39 track detector film alternatively placed at the cell sample position. Fig. 4(a) displays a CR-39 image (after KOH chemical etching) indicating the proton distribution. The large circular white region, whose diameter matches that of the cell capsule aperture, is induced by proton bombardment. Cancer cells were located on the center of this proton irradiation field as indicated by the red circle (5 mm in diameter) in the figure. The areal distribution profile is determined by counting the number of proton-induced etch-pits (tracks) with a microscope along the

horizontal (A-B) and vertical (C-D) lines of Fig. 4(a). The distribution of proton areal density is displayed as dots in Fig. 4(b) and (c) in units of $10^5/\text{mm}^2$ for the A-B and C-D lines, respectively. The nonuniform areal proton density distribution is observed as a tilt. After the first ten of twenty shots the cell capsule was therefore rotated by 180° to reduce this nonuniformity. A more uniform density distribution ($\sigma_{area} = 8.0\%$) was achieved by the rotation as seen in the solid lines of Fig. 4(b) and (c) for the A-B and C-D lines, respectively.

3. Proton dose

The absorbed dose D integrated over n bunches is determined by the following equation:

$$D[\text{Gy}] = n \int_{\varepsilon_0} d\varepsilon_0 \cdot \frac{C \cdot N(\varepsilon_0) \cdot E_d(\varepsilon_0)}{Q \Delta x} \cdot 1.602 \times 10^{-7}. \quad (1)$$

Here $C = 7.20 \times 10^4 \text{ mm}^{-2}$: the averaged density of proton number cross-checked by TOF and CR-39 detectors, $Q = 1 \text{ g/cm}^3$: the mass density of liquid water and $\Delta x = 5 \mu\text{m}$: the thickness of the cell monolayer. ε_0 is the proton energy in vacuum (*i.e.* before entering the thin-foil window) and $N(\varepsilon_0)$ is the normalized energy distribution of protons satisfying $\int N(\varepsilon_0) d\varepsilon_0 = 1$. We determine $N(\varepsilon_0)$ from the averaged TOF spectrum seen in Fig. 3(a, b). $E_d(\varepsilon_0)$ is the energy that is deposited in the cell layer (in keV units) by protons with energy ε_0 . The dynamics of energy deposition are simulated with the 3-dimensional (3D) Monte-Carlo TRIM code [12]. We calculate the energy loss of protons in a multilayer target consisting of the $7.5\text{-}\mu\text{m}$ -thick polyimide window, 3-mm of air, the $7.5\text{-}\mu\text{m}$ -thick polyimide cell dish and $5\text{-}\mu\text{m}$ of liquid water (assumed to be equivalent to the cell monolayer). Typically, protons of $\varepsilon_0 = 2.25 \text{ MeV}$ are decelerated down to 1.9 MeV at the entrance of cell layer. From Eq. (1), the single bunch dose is estimated to be 0.2 Gy corresponding to a single bunch dose rate of 10^7 Gy/s . At the 1 Hz repetition-rate this amounts to a duty factor of 2×10^{-8} with an average dose rate of 0.2 Gy/s. We estimate the statistical error of the integrated proton dose (n shots) according to be

$$\Delta D = D \sqrt{(\sigma_{fluc}^2 + \delta^2)/n + \sigma_{area}^2} \quad (2)$$

where the first standard deviation, σ_{fluc} (12.9%) is the shot-to-shot fluctuation of proton number, the second one, δ (10.5%) is its long term drift and the third one, σ_{area} (8.0%) is the areal proton density fluctuation. The statistical error decreases with the increasing number of proton shots n . We obtain $\Delta D = 9.6\%$ for 2 Gy ($n=10$) and $\Delta D = 8.4\%$ for 8 Gy ($n=40$).

The proton LET (linear energy transfer) in the cell monolayer is evaluated with the 3D TRIM code. We obtain a volume-averaged

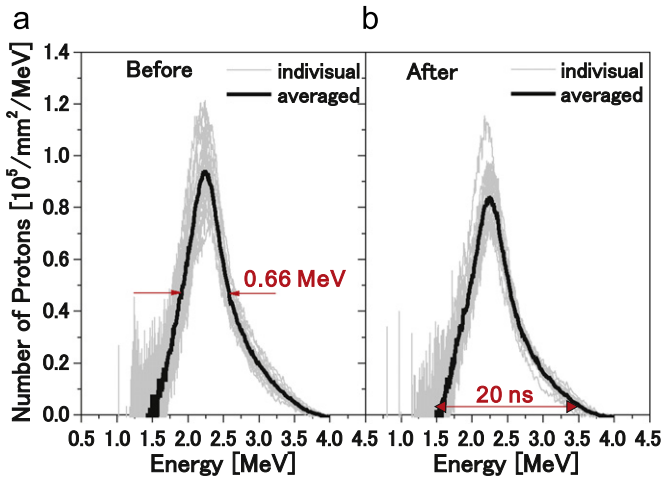


Fig. 3. Energy spectra of protons monitored before (a) and after (b) cell irradiation.

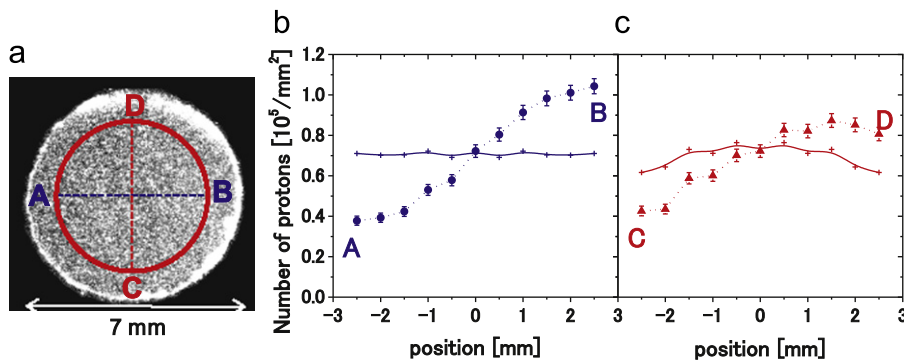


Fig. 4. (a) A beam-spot image near the cell sample position (red circle) measured with CR-39. (b,c) A proton areal densities along the axes, A-B and C-D, respectively, of (a). The proton distributions used for the cell irradiation using the 180° cell rotation are shown with solid lines. (For interpretation of the references to colour in this figure legend, the reader is referred to the web version of this article.)

LET which is

$$LET = \int_{\mathcal{E}_0} d\mathcal{E}_0 \frac{N(\mathcal{E}_0) \cdot E_d(\mathcal{E}_0)}{\Delta x}. \quad (3)$$

Taking into account the proton energy spread of 0.66 MeV (FWHM), the LET is determined to be 17.1 ± 2.8 keV/ μm .

4. Summary

We have developed a laser-driven quasi-monoenergetic proton beamline that consists of four miniature dipole magnets. Laser pulse intensities at the 5×10^{19} –W/cm² level provide the source and acceleration field for protons that are subsequently transported by four energy-selective dipole magnets. The transport line delivers 2.25 MeV protons to the cells with an energy spread of 0.66 MeV. The single bunch dose was 0.2 Gy corresponding to a single bunch dose rate of 10^7 Gy/s. At the 1 Hz repetition-rate this amounts to a duty factor of 2×10^{-8} with an average dose rate of 0.2 Gy/s. The statistical error of the integrated proton dose was 8.4% in standard deviation for 8-Gy (40 shots).

Acknowledgment

This work is supported by Special Coordination Funds for Promoting Science (SCF) commissioned by the Ministry of Education, Culture, Sports, Science and Technology (MEXT) of Japan.

References

- [1] R.R. Wilson, *Radiol.* 47 (1946) 487.
- [2] G. Kraft, M. Scholz, U. Bechtold, *Radiat. Environ. Biophys.* 38 (1999) 229.
- [3] S.V. Bulanov, T.Zh. Esirkepov, V.S. Khoroshkov, A.V. Kuznetsov, F. Pegoraro, *Phys. Lett. A* 299 (2002) 240.
- [4] A. Yogo, K. Sato, M. Nishikino, M. Mori, T. Teshima, H. Numasaki, M. Murakami, Y. Demizu, S. Akagi, S. Nagayama, K. Ogura, A. Sagisaka, S. Orimo, M. Nishiuchi, A.S. Pirozhkov, M. Ikegami, M. Tampo, H. Sakaki, M. Suzuki, I. Daito, Y. Oishi, H. Sugiyama, H. Kiriya, H. Okada, S. Kanazawa, S. Kondo, T. Shimomura, Y. Nakai, M. Tanoue, H. Sasao, D. Wakai, P.R. Bolton, H. Daido, *Appl. Phys. Lett.* 94 (2009) 181502.
- [5] A. Yogo, in: *Proceedings of IPAC10, Kyoto, Japan, 91, 2010*.
- [6] S.D. Kraft, C. Richter, K. Zeil, M. Baumann, E. Beyreuther, S. Bock, M. Bussmann, T.E. Cowan, Y. Dammene, W. Enghardt, U. Helbig, L. Karsch, T. Kluge, L. Laschinsky, E. Lessmann, J. Metzkes, D. Naumburger, R. Sauerbrey, M. Schurer, M. Sobiella, J. Woithe, U. Schramm, J. Pawelke, *New J. Phys.* 12 (2010) 085003.
- [7] T.E. Schmid, G. Dolliger, A. Hauptner, V. Hable, C. Greubel, A. Auer, A.A. Friedl, M. Molls, B. Röper, *Radiat. Res.* 172 (2009) 567.
- [8] M. Nishiuchi, H. Sakaki, T. Hori, P.R. Bolton, K. Ogura, A. Sagisaka, A. Yogo, M. Mori, S. Orimo, A.S. Pirozhkov, I. Daito, H. Kiriya, H. Okada, S. Kanazawa, S. Kondo, T. Shimomura, M. Tanoue, Y. Nakai, H. Sasao, D. Wakai, H. Daido, K. Kondo, H. Souda, H. Tongu, A. Noda, Y. Iseki, T. Nagafuchi, K. Maeda, K. Hanawa, T. Yoshiyuki, T. Shirai, *Phys. Rev. ST Accel. Beams* 13 (2010) 071304.
- [9] H. Kiriya, M. Mori, Y. Nakai, T. Shimomura, H. Sasao, M. Tanoue, S. Kanazawa, D. Wakai, F. Sasao, H. Okada, I. Daito, M. Suzuki, S. Kondo, K. Kondo, A. Sugiyama, P.R. Bolton, A. Yokoyama, H. Daido, S. Kawanishi, T. Kimura, T. Tajima, *Opt. Lett.* 35 (2010) 1497.
- [10] W. Luo, E. Fourkal, J. Li, C.-M. Ma, *Med. Phys.* 32 (2005) 794.
- [11] S. Nakamura, Y. Iwashita, A. Noda, T. Shirai, H. Tongu, A. Fukumi, M. Kado, A. Yogo, M. Mori, S. Orimo, K. Ogura, A. Sagisaka, M. Nishiuchi, Y. Hayashi, Z. Li, H. Daido, Y. Wada, *Jpn. J. Appl. Phys. Part 2* (45) (2006) L913.
- [12] J.F. Ziegler, J.P. Biersack, M.D. Ziegler, *SRIM—The stopping and Range of Ions in Matter*. SRIM Co., 2008.